Synchronization of GAMs and Magnetic Fluctuations on HL-2A tokamak

L.W. Yan[1], K.J. Zhao[1], Y. Nagashima[2], P.H. Diamond[3], J.Q. Dong[1,4], J. Cheng[1], K. Itoh[5], S.-I. Itoh[2], A. Fujisawa[2], S. Inagaki[2], Y. Kosuga[2], M. Sasaki[2], Z. X. Wang[6], L. Wei[6], Z.H. Huang[1], Q. Li[1], X.Q. Ji[1], Y. Huang[1], X.M. Song[1], Yi Liu[1], Q.W. Yang[1], X.T. Ding[1], X.R. Duan[1], Yong Liu[1] and HL-2A team

[1]*Southwestern Institute of Physics, P. O. Box 432, Chengdu 610041, China*
[2]*Research Institute for Applied mechanics, Kyushu University, Kasuga 816-8580, Japan*
[3]*CMTFO, University of California at San Diego, California 92093, USA*
[4]*Institute for Fusion Theory and Simulation, Zhejiang University, Hangzhou* 310027, *China*
[5]*National Institute for Fusion Science, Toki 509-5292, Japan*
[6] *SPOT, Dalian University of Technology, Dalian 116024, China*

E-mail address of contact author: lwyan@swip.ac.cn

The synchronization of geodesic acoustic modes (GAMs) and magnetic fluctuations is identified in the edge plasmas of the HL-2A tokamak for the first time. The frequency entrainment and phase lock are elucidated. Meso-scale electrostatic fluctuations (MSEFs) with components of the dominant GAMs and the m/n = 6/2 potential fluctuations are found to have the same frequency as magnetic fluctuations of m/n = 6/2. The temporal evolutions of the MSEFs and magnetic fluctuations clearly show the frequency entrainment between the GAMs and the m/n = 6/2 magnetic fluctuations. The phase lock between GAMs and magnetic fluctuations is also demonstrated. The results suggest that the GAMs and magnetic fluctuations can transfer energy between each other through nonlinear synchronization. The nonlinear synchronization may contribute to the LFZF (low frequency zonal flow) formation, reduction of turbulent level, and thus confinement regime transitions.

Key words: Geodesic acoustic mode, Magnetic island, Meso-scale electric fluctuation.

The interaction of magnetic field structures and flows in magneto-hydrodynamics is a subject of general interest in physics. Typical examples include magnetic braking of stellar rotation [1], angular momentum transport in astrophysical disks [2, 3], and dynamics of the earth core and geodynamo [4]. In fusion plasmas, the interactions between plasma flows and magnetic fluctuations have attracted much attention, for understanding and control of plasma confinement and transport. For example, the neoclassical tearing modes (NTMs), which need a seed magnetic island for onset [5, 6], can be, theoretically, triggered by a turbulence noise source [7]. Meanwhile, the magnetic island-induced sheared flows can suppress turbulence

and contribute to the formation of an internal transport barrier [8]. The coupling of torioidal Alfven eigenmodes (TAEs) and Beta induced Alfen eigenmodes (BAEs) to the zonal flows is predicted to decrease the saturation level of TAEs and BAEs so as to reduce fast ion loss [9]. For the mitigation/suppression of the large edge localized modes (ELMs) in the H-mode plasmas, which is considered to be an urgent task for fusion researches, the resonant magnetic perturbations (RMPs) [10] are used worldwide. In applying RMPs, the interactions among magnetic perturbations, zonal flows [11], and microscopic turbulence often take place.

Two types of zonal flows, i.e., the low-frequency zonal flows (LFZFs) [11, 12] and the geodesic acoustic modes (GAMs)[13, 14], are known. Effects of magnetic perturbation on zonal flows were routinely reported. For instance, the GAM is damped in the presence of RMPs [15]; the RMP-induced magnetic islands can enhance the LFZFs and turbulence at their boundary [16]; the poloidal flows are reversed when the RMP-induced island width is large enough [17]; a quasi-coherent mode is detected near the low safety factor rational surface [18, 19]. However, the dynamical and mutual interaction between flows and magnetic perturbations has not been deeply studied experimentally.

To understand the complicated interaction of the flows with the magnetic structures, we have to know the ways of their interaction dynamically. Here, the first observation of the synchronization, a universal nonlinear phenomenon in nature [20–22], of GAMs and magnetic fluctuations in the edge plasmas of the HL-2A tokamak is reported. The frequency entrainment and phase lock, two essential elements in synchronization, are demonstrated. Because the magnetic field and velocity field are the two essential vector fields in plasmas, governing the turbulent structure formation in the universe and laboratory, the discovery of synchronization reveals a new, essential and prototypical process in nonlinear dynamics of high temperature plasmas.

The experiments presented here were conducted in Ohmic and ECRH deuterium plasmas of a circular cross section in the HL-2A tokamak. The major and minor radii of the HL-2A tokamak are R = 1.65 m and a = 0.40 m, respectively. The ECRH power is ~500 kW. The parameters specially set for the experiments are the toroidal magnetic field B_t = 1.2-1.3 T, the plasma current I_p = 150-180 kA, the line

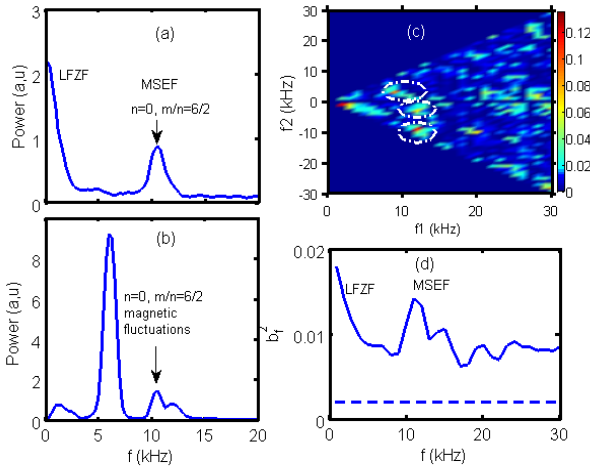

Figure 1. The auto-power spectra of the floating potential fluctuations (a), magnetic fluctuations (b), squared bicoherence (c), summed bicoherence (d).

averaged electron density n_e = 1-2×$10^{19}$$m^{-3}$, the safety factor q_a = 3.3. The sampling rate of the probe data is 1 MHz, corresponding to Niquist frequency of 500 kHz. The frequency resolution is 0.25 kHz in the following analysis unless otherwise stated. A combination of distributed Langmuir probe (LP) arrays was used to measure floating potential fluctuations and Mach number. In the combination, a LP array of 3 tips and a four-tip LP array form a fast reciprocating probe set of 7 tips with a 65 mm poloidal span. A radial rake probe array of 12 tips, in the toroidal direction, is located in the poloidal cross section ~2100mm away from the set of 7 tips. It was used to get profiles of floating potential fluctuations. The tip size and the mount of the LP sets are the same as was described in Ref. [23]. The meso-scale electric fluctuations (MSEFs) with components of the dominant GAMs (n=0) and the m/n=6/2 potential fluctuations are detected inside the last closed flux surface (LCFS) in ECRH plasmas. The tips are located at the radial position of $\Delta r = -4.6$ cm, where the minus sign means inwards from the LCFS. Figure 1 presents the auto power spectra of the floating potential fluctuations and the magnetic fluctuations from the Mirnov coils set up on the vacuum vessel wall, respectively. The small peak shown in the figure 1(a) at the frequency of ~10.5 kHz is the MSEF. A large power fraction peak of the LFZF in the frequency range of 0.25-3 kHz is also detected. The large peak at the frequency of ~6 kHz shown in figure 1(b) is the tearing modes with mode numbers of m/n = 2/1. The small peak presented in figure 1(b) at the same frequency as the MSEFs has components of the dominant m/n = 6/2 magnetic fluctuations and the n = 0 zonal field. Besides, the two small peaks at the frequency of 1.2 kHz and 12 kHz come from the power supply and the m/n = 4/2 tearing mode, respectively.

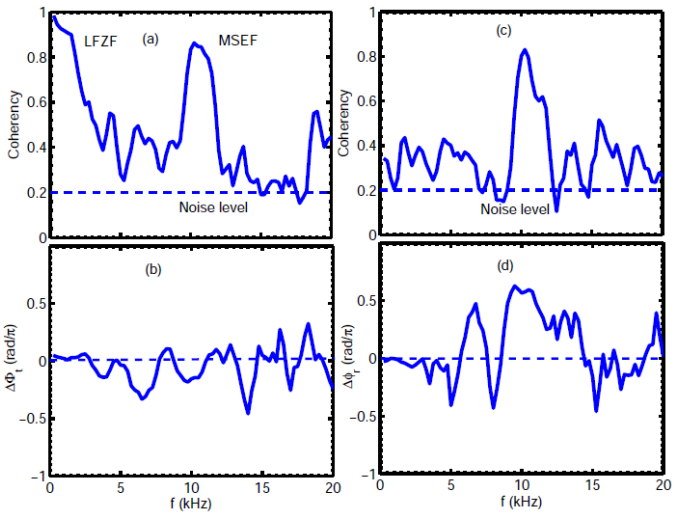

Figure 2. (a) The toroidal coherency between potential fluctuations, and (b) its phase shifts, (c) the coherency between floating potential and magnetic fluctuations, and (d) the radial phase shift between potential fluctuations.

The interaction between LFZFs and MSEFs is an important physics issue associated with LFZF formation mechanism. The bicoherence analysis, an indicator for the strength of nonlinear three wave coupling, can prove the existence of the interaction between LFZFs and MSEFs. The squared auto-bicoherence $b_f^2 = |B(f)|^2 / <|\phi_f(f_1)\phi_f(f_2)|^2><|\phi_f(f)|^2>$ of the perturbations is calculated. Here the

bispectrum $B(f) = < \phi_f(f_1)\phi_f(f_2)\phi_f^*(f = f_1 \pm f_2) >$, where < > denotes an ensemble average. The frequency resolution is 1 kHz, the number of realization is M = 472, and the noise level is 0.002 for the analysis. Figure 1(c) plots the squared auto-bicohence of the floating potential fluctuations in the low frequency region of $f_1 < 30$kHz, and $f_2 = -30 - +30$kHz. The bicoherence in the frequency region (dash-dotted ellipse) of $f_1 = 9-14$kHz, $f_2 = 0-\pm 5$kHz, and $f = f_1 + f_2 = 0 - 5$kHz is significantly above the noise level. This analysis suggests that the MSEFs may contribute to the LFZF formation through the nonlinear three wave coupling between MSEFs and LFZFs. The summed bicoherence is shown in figure. 1(d). The peaks in the LFZF and MSEF frequency regions indicate that LFZFs and MSEFs can also interact with the turbulence.

Figures 2 shows the toroidal coherency between potential fluctuations, their phase shifts, the coherency between floating potential and magnetic fluctuations, and the radial phase shifts between potential fluctuations, respectively. Here, the coherency is described as $C_{xy}(\tau) = < x_i - \bar{x} >< y_i - \bar{y} > / \sqrt{< (x_i - \bar{x})^2 >< (y_i - \bar{y})^2 >}$, where X_i and Y_i are two sets of variables, i stands for time series, and <…> denotes an ensemble average, corresponding to $\bar{x}$, $\bar{y}$. The toroidal coherency in the LFZF and MSEF frequency bands is all quite high. This indicates that the MSEF and LFZF have strong correlation in toroidal direction with a span of 2100 mm. The corresponding phase shift in the MSEF frequency region is estimated as $\Delta\phi_t$ = 0.25 ±0.09 rad. The toroidal mode number is calculated as $\Delta n = 0 \pm 0.2$. The evaluated radial phase shift is $\Delta\phi_r = 1.4 \pm 0.2$ rad, and the corresponding radial wave vector is estimated as $k_r = 3.5 \pm 0.2$ cm^{-1} with the span of 4 mm in radial direction. Thus, we conclude that the MSEF has the characteristics of the toroidal symmetries, and finite radial wave numbers, and thus the GAM component

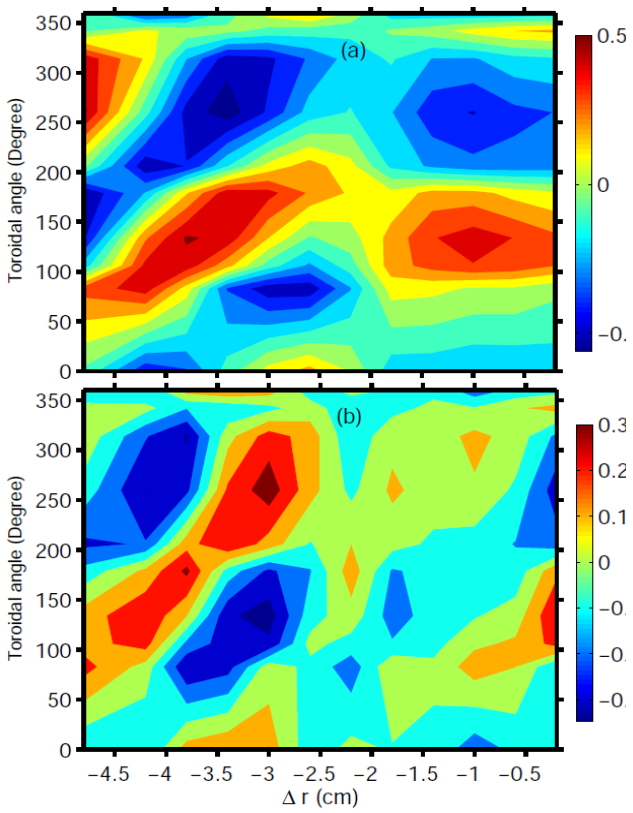

Figure 3. The contour plots of coherency between potential and magnetic fluctuations (a), and between turbulent envelope and magnetic fluctuations in the frequency band of 9-11kHz (b).

is dominant. In addition, the calculated coherency between the MSEFs and the magnetic fluctuations at the MSEF frequency is significantly above the noise level, indicating that the MSEFs are well correlated with the magnetic fluctuations.

The spatial structures of the MSEF at the frequency of ~10.5 kHz were identified with correlation analysis further. Figure 3 (a) shows the contour of C(X(Δr), Y(Δξ)), where X(Δr) is the potential perturbation at r = a+Δr and Y(ξ) is the magnetic fluctuation measured with the Mirnov coil at the toroidal angle ξ. The 12 probe tips are uniformly distributed in the radial direction from -4.8 to -0.4 cm inside the LCFS. The 10 Mirnov coils are located at different toroidal angles. The toroidal mode number of n = 2 is clearly demonstrated for the potential fluctuation at the frequency of ~ 10.5 kHz. The poloidal mode number of m = 6 is also estimated with similar analysis. Figure 3(b) also gives the contour plot of the coherency between turbulence envelopes and magnetic fluctuations. The poloidal and toroidal mode numbers for the turbulence envelope are identified as m = 6 and n = 2, respectively. This analysis indicates that the MSEF contains m/n = 6/2 potential fluctuations. The phase shift between the turbulence envelope and the m/n = 6/2 potential fluctuation is close to π/2. The radial wavelengths of the m/n = 6/2 potential fluctuation and turbulence envelope are all estimated as about ~ 2 cm. The m/n = 6/2 potential fluctuation propagates in the directions of toroidal magnetic field and ion diamagnetic drift.

The radial distributions of the potential fluctuation power at the MSEF frequency are measured and shown in figure 4 (a). The power as a function of the radial position shows two peaks. The amplitude of the MSEF first increases from the LCFS inwards, but reduces at the position of Δr~ -2.0 cm, where the surface of the safety factor q = 3 is located. Then the power increases and reaches a maximum at Δr~ -3.0 cm again. After that, the power deceases inwards. The profiles of the phase shift between the MSEFs and the magnetic fluctuations by Fast Fourier Transformation analysis is also provided in figure

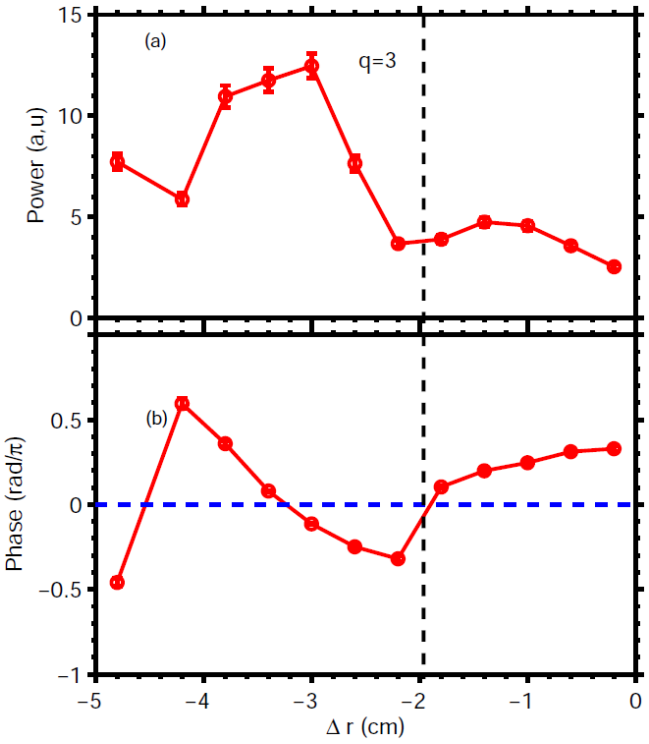

Figure 4. The radial profiles of MSEF power (a), and (b) the phase shifts between potential and magnetic fluctuations of m/n=6/2.

4(b). The sign of the phase shift changes at Δr~ -2.0 cm, indicating that the sign of the MSEF inverts at the q = 3 surface. The reduction of the MSEF and the change of the sign for the MSEF around q = 3 surface may come from the m/n = 6/2 islands. The radius of q = 3 surface is estimated by magnetic measurements.

In order to understand the interaction mechanism of the GAMs and the magnetic fluctuations, the temporal evolutions of the MSEFs and magnetic fluctuations of m/n = 6/2 are investigated [24]. Figure 5(a) shows the spectrogram of the floating potential fluctuations in the MSEF frequency range at the radial position of Δr = -3.0 cm. In the period of 500 - 530 ms, the MSEF frequency rapidly decreases from 15.5 kHz to 12.5 kHz. At the beginning of the ECRH, the MSEF is located at the frequency of ~ 12.5 kHz, and its frequency decreases continuously. After ~ 590 ms, the MSEF frequency becomes stable and is about 10.5 kHz. Figure 5 (b) also gives the spectrogram of the m/n = 6/2 magnetic fluctuations. The m/n = 6/2 magnetic fluctuations follow the MSEF frequency and its intensity increases gradually. After the ECRH switching off at ~ 650 ms, the MSEF frequency decrease again and no significant magnetic fluctuation is observed at the MSEF frequency. The result suggests that the frequency entrainment of the GAM and the m/n = 6/2 magnetic fluctuations exists.

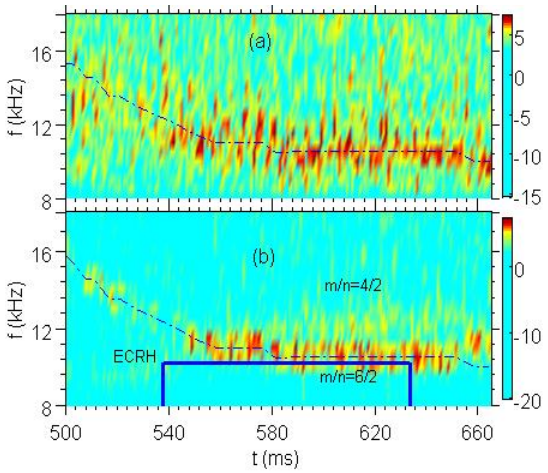

Figure 5. The spectrograms of the MSEFs (a) and magnetic fluctuations of m/n=6/2 (b). The dash-dotted line is center of MSEF frequency.

The phase lock is another important evidence to prove the frequency entrainment linked to the nonlinear synchronization of GAMs and magnetic fluctuations. Figure 6 shows the probability distribution function (PDF) of the phase shifts between MSEFs and magnetic fluctuations at different time slices. The phase shifts are estimated with the Hilbert transition. Before the ECRH, peaks are clearly shown at different time regions. This indicates that their phases are locked. After ECRH switching on, the peaks become stable and the half width of the peaks becomes narrow, especially, during the periods of 590-600 ms and 600-610 ms. After ECRH switching off, the half width of the peaks becomes wider and the peak disappears gradually. This result suggests that the phase shifts between GAMs and magnetic fluctuations are locked through adjusting their phases via nonlinear interaction. The m/n = 3/1 basic harmonic mode is not observed in the present experiments. This indicates that the m/n = 6/2 mode does not come from the m/n=3/1 basic harmonic mode. The turbulence-

driven GAMs has close frequency with m/n = 6/2 magnetic fluctuations. The synchronization of GAMs and magnetic fluctuations suggests that GAMs and magnetic fluctuations can transfer energy between each other through nonlinear synchronization. Therefore, the observation suggests that synchronization might contributes to the excitation of m/n = 6/2 magnetic fluctuations. This cannot be understood by the present theory. In this experiment, we also observed that the MSEFs interact with LFZFs and turbulence, suggesting that the synchronization contributes to the LFZF formation, and thus reduces turbulence level. The LFZF is favorable for the L-H transitions. Thus, we speculate that the synchronization can contribute to confinement regime transitions, especially L-H transitions [25].

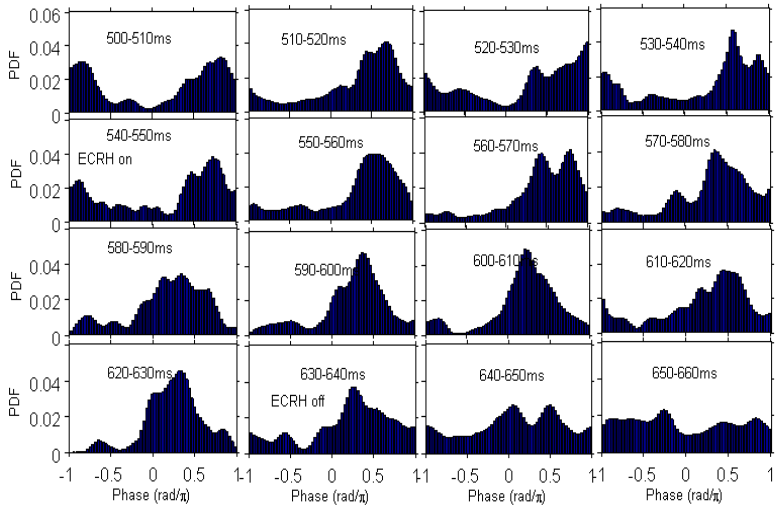

Figure 6. The probability distribution functions (PDFs) of phase shifts between the MSEFs and magnetic fluctuations at different time slices.

In summary, the synchronization of GAMs and magnetic fluctuations is observed for the first time in the edge plasmas of the HL-2A tokamak using multiple Langmuir probe arrays. This is the discovery of the new and essential structure formations of plasmas, in which the two fundamental vector-fields (magnetic field and flow field) couple dynamically.

This work is partially supported by National Science Foundation of China, Nos. 11175060, 11175058, 11375054, 91130031, and 11320101005; by the National Magnetic Confinement Fusion Science Program No.2013GB107001, 2014GB107000 and 2013GB112008; by the China-Korean joint foundation under the grant No. 2012DFG02230, by the U.S. Department of Energy (DOE) under Award Number DE-FG02- 04ER54738 and CMTFO; and Grant-in-Aid for Scientific Research of JSPS (15H02155, 15H02335, 23244113).

References

[1] Matt Seanp, et al., APJ, 754, L26 (2012).

[2] S. A. Balbus and J. F. Hawley, APJ, 376, 241(1991).

[3] S. A. Balbus and J. F. Hawley, Rev. Mode. Phys, 70, 1,(1998).

[4] J. Aubert and A. Fournier, Nonlin. Processes Geophys, 18, 657(2011).

[5] D. Biskamp, Magnetic Reconnection in Plasmas, (Cambridge University Press, Cambridge, England, 2000).

[6] P. K. Kaw, E. J. Valeo, and P. H. Rutherford, Phys. Rev.Lett. 43, 1398 (1979).

[7] S-I. Itoh, K. Itoh, and M. Yagi, Phys. Rev. Lett. 91, 045003 (2003).

[8] T. Estrada et al, Nucl. Fusion, 47, 305 (2007).

[9] Z. Lin et al., 25th IAEA fusion conference, TH/7-2, 13-18 October 2014, Saint Petersburg, Russia.

[10] T. E. Evans et al., Phys. Rev. Lett. 92, 235003 (2004).

[11] A. Hasegawa et al., Phys. Rev. Lett. 59, 1581 (1987).

[12] P. H. Diamond et al., Plasma Phys. Control. Fusion 47, R35 (2005).

[13] N. Winsor et al., Phys. Fluids 11, 2448 (1968).

[14] K. J. Zhao et al., Phys. Rev. Lett. 96, 255004 (2006)

[15] J. R .Robinson et al., Plasma Phys. Control. Fusion 54, 105007 (2012).

[16] K. J. Zhao et al., Nucl. Fusion 55, 073022 (2015).

[17] K. Ida, et al., Phys. Rev. Lett. 88, 015002 (2002).

[18] H. W. Y. Tsui et al., Phys. Rev. Lett. 70, 2565 (1993).

[19] H. W. Y. Tsui et al., Phys. fluids B 5, 1274 (1993).

[20] L. M. Pecora and T. L. Carroll, Phys. Rev. Lett. 64, 821 (1990).

[21] A. Pikovsky, et al., Synchronization. A Universal Concept in Nonlinear Science, (Cambridge University Press, Cambridge, England, 2001).

[22] J. A. Acebr´on et al., Rev. Mod. Phys 77, 137(2005).

[23] K. J. Zhao et al., Plasma Phys. Control. Fusion 52, 124008 (2010).

[24] K. J. Zhao, et al. Phys. Rev. Lett. 117 (2016), in press

[25] L.W. Yan, et al. Nucl. Fusion 55, 073026 (2015).